Aquachlororuthenium(III) catalysis in the oxidation of substituted 4-oxo-4-arylbutanoic acids by bromate in acid medium: a kinetic and mechanistic study and validity of linear free-energy relationships

Padma Sunitha Manjari · Cherkupally Sanjeeva Reddy

Abstract Ru(III) acts an efficient catalyst in the oxidation of substituted 4-oxo-4-arylbutanoic acids (4-oxo acids) by bromate in sulfuric acid medium, giving the corresponding benzoic acids in quantitative yields. The reaction shows first-order dependence in both [bromate] and [H$_2$SO$_4$], and a non-linear dependence on both [oxo acid] and [catalyst]. Changing solvent from H$_2$O to D$_2$O increases the rate. The rate is not affected by ionic strength but decreases with increase in dielectric constant of the medium. Electron-releasing substituents in the phenyl ring of the substrate greatly accelerate the rate, whereas the retardation by electron-withdrawing substituents, though perceptible, is small. The linear free-energy relationship is characterized by smooth curves in Hammett plots of log k versus σ; however, linear plots are obtained with excellent correlation coefficients at all the studied temperatures, when Brown's σ^+ values are used. The reaction constant is negative and decreases with increase in temperature. From the intersection of the lines in the Hammett and Arrhenius plots, the isokinetic relationship is evaluated. A mechanism involving a cyclic oxidant–substrate–catalyst ternary complex is proposed, in which both C–C bond-breaking and C–O bond formation are involved, and the oxidation state of Ru(III) remains unchanged. A rate law explaining all the kinetic results has been derived and verified. The reaction is an example of neighboring group participation in intramolecular catalysis and is potentially useful for the synthesis of substituted benzoic acids.

P. S. Manjari · C. S. Reddy (✉)
Catalysis Laboratory, Department of Chemistry, University College, Kakatiya University, Warangal 506009, India
e-mail: chsrkuc@yahoo.co.in

Introduction

The carbonyl and carboxy groups of 4-oxo-4-phenylbutanoic acid and its phenyl substituted compounds (commonly known as 4-oxo acids) are separated by two carbons; hence, the two functional groups are essentially independent. However, an intramolecular mechanism in the catalytic iodination of 4-oxo acid [1] and neighboring group participation in the hydrolysis of its ethyl ester [2, 3] has been reported. In acidic medium 4-oxo acids undergo enolization [4], and on selective oxidation, they result in malonic and substituted benzoic acids, which find widespread applications in synthetic organic chemistry. Hence, 4-oxo acids are attractive substrates in terms of their mechanistic aspects.

Sodium and potassium bromate are stable solids and can be easily handled when compared with liquid bromine and hypobromous acid solutions. The product of bromate oxidation is bromide, which can be safely recycled, thus making bromate oxidations environmentally benign compared with metal ion oxidations. Though bromate itself is a strong oxidizing agent, having a redox potential of 1.45 V [5], the oxidations generally require a catalyst. Ru(III) has been used as a homogeneous catalyst in many redox reactions and its versatility as a catalyst is revealed by oxidation studies of various organic substrates involving different oxidants [6–10]. The mechanism of catalysis is often quite complicated due to the formation of different intermediate complexes, free radicals and oxidation states of Ru.

Our preliminary experimental results indicated that the reaction of 4-oxo acids with bromate in acid medium without a catalyst is sluggish, but accelerated by a small amount of RuCl$_3$ catalyst. Therefore, in order to explore the mechanism of oxo acid–bromate reactions and also to

study the catalytic action of Ru(III), we chose RuCl$_3$ as a catalyst. While studying the present reaction in the presence of mercury(II), a bromo-complexing metal ion, some interesting results were obtained. Ru(III)-catalyzed bromate oxidation of malonic acid (MA) and methyl malonic acid (MMA) exhibit an induction period [11], whose duration is inversely proportional to [substrate], [catalyst] and [acid], and independent of [bromate]. After induction, the reaction is first order in both [bromate] and [catalyst] but shows less than unity order in [substrate] and an inverse fractional order in [acid]. However, the present reaction does not show any induction period over a wide concentration range of bromate, Ru(III), oxo acid and H$_2$SO$_4$. The kinetic behavior of the present reactants and catalyst is entirely different from the earlier reports of Ru(III)-catalyzed oxidation reactions [6–11]. The mechanism neither resembles catalysis by bromide anions [12] nor that of Ru(III)-catalyzed oxidation of organic substrates with the oxidants [6–11].

In the present study, we describe the kinetics and mechanism of oxidation of substituted 4-oxo-4-arylbutanoic acids by bromate in sulphuric acid medium containing mercury(II) and Ru(III), including the active species of the substrate, catalyst and oxidant, and the oxidation products. We have also studied the catalytic efficiency of Ru(III) and evaluated the related kinetic and thermodynamic parameters of the reaction, along with the linear free-energy and isokinetic relationships.

Experimental

All the oxo acids were obtained from Aldrich and recrystallized twice from water before use. The purity of substrates was checked by their melting points, UV, IR and NMR spectra. KBrO$_3$ (Reidal), H$_2$SO$_4$ and Hg(OAc)$_2$ (Merck) were of analytical reagent grade and used as received. D$_2$O (99.4% pure) was obtained from the Baba Atomic Research Centre, Mumbai, India. Acetic acid (BDH) was purified by refluxing with chromic acid and acetic anhydride for 6 h and then distilled. Ruthenium trichloride hydrate (Johnson Matthey) was purified by evaporation with conc. HCl. A stock solution of Ru(III) was prepared by dissolving a weighed quantity of RuCl$_3$ in dilute HCl of known strength. Mercury was added to this solution, to detect the formation of any Ru(IV) during its preparation, and the solution was kept for 1 day. The obtained solution was assayed by EDTA titration [13] and stored in a glass-stoppered flask, painted black, at ∼5 °C. Dilute solutions of Ru(III) were made from the stock solution as required. Other solutions were prepared with either doubly distilled water or purified acetic acid and were standardized by known methods. Separation and

identification of organic intermediates in the reaction were performed using HPLC. The experiments were performed with a Shimadzu instrument using an ion-exchange column at 45 °C and a UV detector working at 220 nm. The intermediates and products were identified from their retention time (t_r). A Shimadzu multipurpose recording double beam UV–visible spectrophotometer equipped with a temperature controller was used for absorption studies.

Kinetic measurements

All the kinetic measurements were carried out in black-coated vessels at constant temperature (±0.1 °C) under pseudo-first-order conditions with [oxo acid] ≫ [bromate]. The reaction was initiated by the rapid addition of temperature-equilibrated oxidant of the required concentration to reaction mixtures containing the required amounts of substrate, catalyst, Hg(OAc)$_2$, H$_2$SO$_4$, AcOH and water, in glass-stoppered Pyrex boiling tubes that were thermally equilibrated for 1 h. The progress of the reaction was monitored by iodometric determination of unconsumed [bromate] in known aliquots of the reaction mixtures at different time intervals. Before adopting the iodometric method, it was ensured that the presence of oxo acid in the quenching solution of KI did not change the bromate titer value. The course of the reaction was studied for at least three half-lives. The rate constants (k, s^{-1}) were determined from the pseudo-first-order plots of log [oxidant] against time. The pseudo-first-order plots were linear ($R^2 \geq 0.99$) for more than 80% completion of the reaction, and the k (s^{-1}) values were reproducible to within ±5%. Rate constants did not alter in a nitrogen atmosphere, and all the rate constants reported in this paper were obtained without nitrogen. Freshly prepared solutions of oxo acids in purified acetic acid were used throughout. The uncatalyzed reaction is very slow under these conditions and is first order in both [bromate] and [oxo acid], and second order in [H$^+$]. However, the reaction rate is appreciably faster (40–80 times) in the presence of a minute quantity (10^{-5} mol dm^{-3}) of RuCl$_3$. All the rate constants for the catalyzed reactions were obtained as: $k_{\text{catalyzed}} = k_{\text{overall}} - k_{\text{uncatalyzed}}$ and represented as k (s^{-1}).

Results

Characterization of the reaction kinetics

Molecular bromine production anticipated from the bromate–bromide reaction and its subsequent reaction with the oxo acid was eliminated by the addition of the bromo-complexing agent Hg(II) [14]. The added mercury acetate had no effect on the rate of reaction over a wide

concentration range (0.001–0.01 mol dm^{-3}). An optimum concentration (0.005 mol dm^{-3}) of mercury acetate was employed throughout; hence, the reported rate constants and thermodynamic parameters pertain to pure bromate (uncontaminated with Br$_2$) oxidation only.

At fixed concentration of other reactants and when [oxo acid] is in tenfold excess over [bromate], the kinetic studies were carried out at different [bromate]$_{init}$ in the range of 5.0–20.0 × 10^{-4} mol dm^{-3}. Linear plots were obtained ($R^2 \geq 0.99$) for log [bromate]$_t$ versus time at all [bromate]$_{init}$ for more than three half-lives of the reaction. The obtained pseudo-first-order rate constant (k, s^{-1}), evaluated from the slopes of such plots, remained unchanged (Table 1), confirming the first-order dependence of the rate on [bromate]$_{init}$.

The effect of [oxo acid] on the reaction rate was studied in the concentration range of 0.005–0.03 mol dm^{-3}, at constant concentrations of oxidant, acid and catalyst (Table 1). The plots of log k versus log [oxo acid] were linear ($R^2 \geq 0.99$) with slope values less than one (0.50–0.54). The plots of k against [oxo acid] were non-linear, but the double reciprocal plots, 1/k against 1/[oxo

Table 1 Dependence of rate on the factors influencing the Ru(III) catalyzed oxidation of 4-oxo acids by bromate in acid medium at 313 K

Non-variable constituents (mol dm^{-3})	Variable constituent (mol dm^{-3})	$10^4 \times k$ (s^{-1})				
		–H	p-OCH$_3$	p-CH$_3$	p-Cl	m-NO$_2$
	[Bromate]					
[Oxo acid] = 1.0 × 10^{-2}	5.0 × 10^{-4}	12.79	115.15	28.78	7.89	1.75
[H$_2$SO$_4$] = 1.0	7.5 × 10^{-4}	12.74	115.09	28.76	7.95	1.75
[Ru(III)] = 3.3 × 10^{-5}	10.0 × 10^{-4}	12.79	115.15	28.78	7.99	1.75
AcOH–H$_2$O = 1:1 (% v/v)	15.0 × 10^{-4}	12.78	115.10	28.77	7.99	1.74
[Hg(OAc)$_2$] = 5.0 × 10^{-3}	20.0 × 10^{-4}	12.81	115.14	28.78	7.94	1.76
	[Oxo acid]					
[Bromate] = 1.0 × 10^{-3}	5.0 × 10^{-3}	9.59	79.94	19.67	5.53	1.07
[H$_2$SO$_4$] = 1.0	7.5 × 10^{-3}	10.99	96.60	23.71	6.91	1.46
[Ru(III)] = 3.3 × 10^{-5}	10.0 × 10^{-3}	12.79	115.15	28.78	7.99	1.75
AcOH–H$_2$O = 1:1 (% v/v)	15.0 × 10^{-3}	15.32	143.91	34.76	9.54	2.18
[Hg(OAc)$_2$] = 5.0 × 10^{-3}	20.0 × 10^{-3}	18.19	169.82	41.22	11.51	2.55
	25.0 × 10^{-3}	19.87	192.75	45.18	12.69	2.87
	30.0 × 10^{-3}	22.90	–	51.16	13.90	3.18
	[Ru(III)]					
[Bromate] = 1.0 × 10^{-3}	1.65 × 10^{-5}	8.47	64.51	20.89	5.24	1.27
[Oxo acid] = 1.0 × 10^{-2}	3.33 × 10^{-5}	12.79	115.15	28.78	7.99	1.75
[H$_2$SO$_4$] = 1.0	6.66 × 10^{-5}	17.75	161.29	43.97	11.51	2.50
AcOH–H$_2$O = 1:1 (% v/v)	9.99 × 10^{-5}	20.98	191.91	52.48	13.90	2.87
[Hg(OAc)$_2$] = 5.0 × 10^{-3}	13.32 × 10^{-5}	25.58	227.72	57.57	15.98	3.46
	[H$_2$SO$_4$]					
[Bromate] = 1.0 × 10^{-3}	0.25	3.22	28.08	9.59	2.36	0.43
[Oxo acid] = 1.0 × 10^{-2}	0.50	6.39	53.71	19.19	4.39	0.92
[Ru(III)] = 3.3 × 10^{-5}	0.75	9.59	83.17	24.21	6.30	1.44
AcOH–H$_2$O = 1:1 (% v/v)	1.00	12.79	115.15	28.78	7.99	1.75
[Hg(OAc)$_2$] = 5.0 × 10^{-3}	1.25	15.89	140.63	46.06	9.59	2.42
	1.50	19.25	172.42	57.57	11.51	2.87
	AcOH–H$_2$O (% v/v)					
[Bromate] = 1.0 × 10^{-3}	30–70 (53.18)[a]	7.67	38.38	16.79	4.79	0.72
[Oxo acid] = 1.0 × 10^{-2}	40–60 (46.48)	9.59	51.15	23.02	6.39	1.53
[Ru(III)] = 3.3 × 10^{-5}	50–50 (39.78)	12.79	115.15	28.78	7.99	1.75
[H$_2$SO$_4$] = 1.0	60–40 (33.08)	19.19	307.04	43.17	9.59	2.68
[Hg(OAc)$_2$] = 5.0 × 10^{-3}	70–30 (26.08)	33.58	–	76.76	13.43	3.83

Reported rate constants are the mean of duplicate experiments

[a] Parentheses values indicate the dielectric constant of the medium

Fig. 1 Plot of $1/k$ against $1/[\text{oxo acid}]$ at 313 K. Reaction conditions as in Table 1. *A* p-OCH$_3$, *B* p-CH$_3$, *C* –H, *D* p-Cl, *E* m-NO$_2$

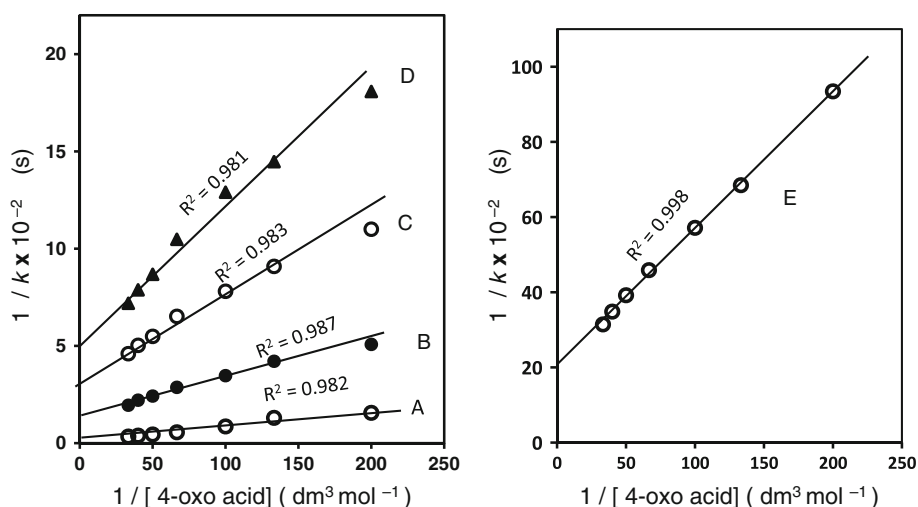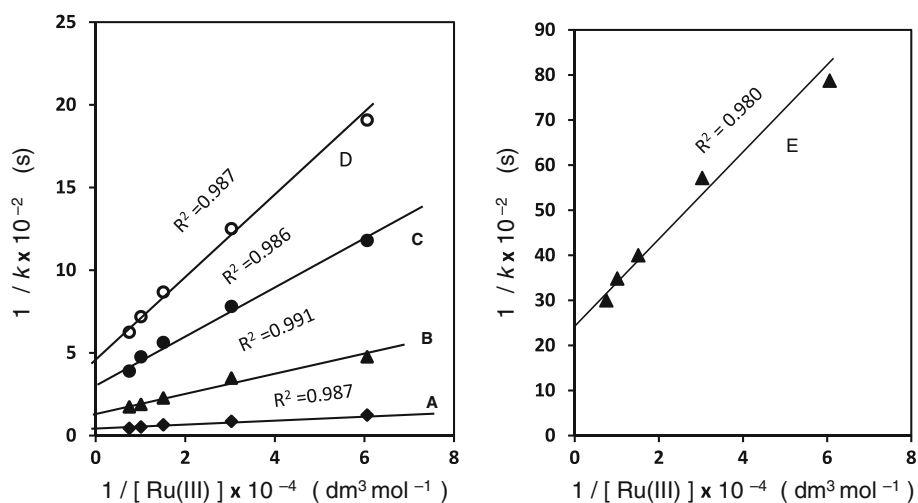**Fig. 2** Plot of $1/k$ against $1/[\text{Ru(III)}]$ at 313 K. Reaction conditions as in Table 1. *A* p-OCH$_3$, *B* p-CH$_3$, *C* –H, *D* p-Cl, *E* m-NO$_2$

acid], were linear with varying intercepts and slopes (Fig. 1), confirming that the order in [oxo acid] varies from one to zero. Under similar experimental conditions, the uncatalyzed reaction, though very slow, was first order with respect to [oxo acid].

The effect of [Ru(III)] was studied between the concentration range of 1.65×10^{-5} and 13.32×10^{-5} mol dm^{-3} (Table 1). The order in [catalyst] was found to be 0.50 ± 0.05 as determined from the slope of log k against log [catalyst] plots, and the plots of k against [catalyst]$^{0.5}$ were linear. Further, plots of $1/k$ versus $1/[\text{Ru(III)}]$ (Fig. 2) were linear with varying intercepts on the $1/k$ axis for the studied oxo acids.

The effect of [H$_2$SO$_4$] on the reaction rate was studied in order to establish the active species of reactants present in the solution. At fixed concentrations of substrate, bromate, catalyst and other conditions remaining constant, the reaction rate increased linearly (Table 1) with increase in [H$_2$SO$_4$] and the order with respect to [H$_2$SO$_4$] was found

to be unity. The plots of $1/k$ versus $1/[\text{H}_2\text{SO}_4]$ were found to be linear passing through the origin (Fig. 3). Under similar conditions, the uncatalyzed reaction was second order with respect to [H$_2$SO$_4$].

The effect of ionic strength was studied using NaClO$_4$, with other experimental conditions held constant. There was no significant effect of ionic strength on the reaction rate; hence, ionic strength of the medium was not fixed at any constant value in the other experiments.

The dielectric constant of the medium was varied using different proportions of acetic acid and water (30–70% v/v). The D values were calculated from the equation

$$D = (D_W V_W) + (D_A V_A)$$

where D_W and D_A are the dielectric constants of pure water and acetic acid, respectively, and V_W and V_A are the volume fractions of components water and acetic acid, respectively in the total mixture. The rate increased with increasing acetic acid content (Table 1). Plots of log k versus $1/D$ were

Fig. 3 Plot between $1/k$ and $1/[H_2SO_4]$ at 313 K. Reaction conditions as in Table 1. A p-OCH$_3$, B p-CH$_3$, C –H, D p-Cl, E m-NO$_2$
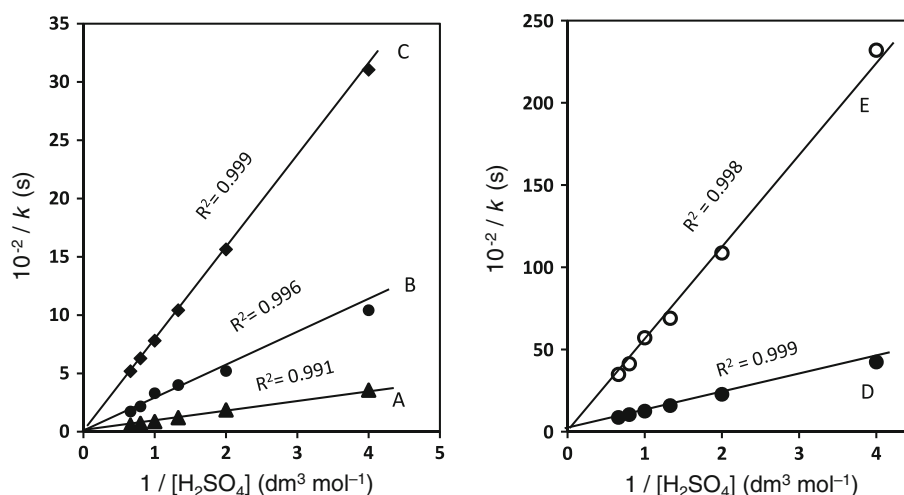
linear with positive slopes. Blank experiments showed that acetic acid was not oxidized by bromate under these conditions. The observed results therefore truly represent the rates under different dielectric medium of the solution.

Effects of conditions and substituents

The reactions were neither accelerated nor retarded by added acrylonitrile (0.1–1.0 mol dm^{-3}) and also no precipitate due to polymerization of acrylonitrile was observed, suggesting the absence of any free radicals in the reaction. To further confirm the absence of free radicals, the reaction was carried out in the presence of 0.05 mol dm^{-3} 2,6-di-t-butyl-4-methylphenol (BHT). The unreacted BHT was recovered almost quantitatively at the end of the experiment.

Rate studies in D$_2$O medium revealed that the reaction rates were faster in D$_2$O than in H$_2$O and $k(H_2O)/k(D_2O) = 0.55 \pm 0.01$ at all the studied temperatures for all the studied oxo acids (Table 2). Since D$_3$O$^+$ is a stronger acid than H$_3$O$^+$ [15], the value of the solvent isotope effect suggests a proton catalyzed oxidation reaction.

The oxidation reactions were studied in the temperature range of 298–323 K keeping all constituents of the solution constant. The experimental rate constant k (which is a composite of the enolization, complexation and oxidation steps) was determined at all the temperatures for all the studied oxo acids (Table 3). Activation energy (E_a) was calculated from the least-square slopes of linear Arrhenius plots of log k versus $1/T$ (Fig. 4a; $R^2 \geq 0.99$). The related thermodynamic parameters, i.e., the enthalpy of activation ($\Delta H^{\#}$), entropy of activation ($\Delta S^{\#}$) and free energy of activation ($\Delta G^{\#}$) were calculated using the appropriate equations and are presented in Table 3. The plot of $\Delta H^{\#}$ against $\Delta S^{\#}$ was linear (Fig. 4b), and the isokinetic temperature (β) obtained is 370.3 K. The value of β calculated from the Exner's plot (Fig. 4c) of log $k_{323\ K}$ against log $k_{313\ K}$ is 370.2 K, which is in good agreement with the value obtained from the $\Delta H^{\#}$ against $\Delta S^{\#}$ plot. The value of β is higher than the experimental temperature range (298–323 K), indicating that the reaction is enthalpy controlled.

The substituent effect on the rate of oxidation was studied using different phenyl substituted 4-oxo acids (ArCOCH$_2$CH$_2$COOH, where Ar = 4-methoxy-, 4-methyl-, 4-chloro- or 3-nitro-substituted phenyl) at different temperatures (Table 3). Structural changes in the phenyl moiety result in varied reactivity; while electron-releasing substituents greatly accelerate the rate of oxidation, the retardation by electron-withdrawing substituents though perceptible was small. The linear free-energy relationship is characterized by a smooth curve in the Hammett plot of log k versus σ at all the studied temperatures (Fig. 5a). However, linear Hammett plots were obtained, with excellent correlation coefficients at all the studied temperatures (Fig. 5b; $R^2 \geq 0.998$), when exalted substituent constants (Brown and Okamoto's σ^+) values [16] were used. The reaction constant is negative and

Table 2 Solvent isotope effect on the rate of Ru(III)-catalyzed bromate oxidation of 4-oxo acids at 313 K

4-oxo acid	$k\ (H_2O) \times 10^4$ (s^{-1})	$k\ (D_2O) \times 10^4$ (s^{-1})	$k\ (H_2O)/ k\ (D_2O)$
–H	12.79	23.02	0.55
p-methyl	28.78	51.22	0.56
p-chloro	7.99	14.53	0.55
m-nitro	1.75	3.24	0.54

Solution conditions: [Oxo acid] = 1.00×10^{-2} mol dm^{-3}, [bromate] = 1.00×10^{-3} mol dm^{-3}, [Ru(III)] = 3.3×10^{-5} mol dm^{-3}, [H$_2$SO$_4$] = 1.00 mol dm^{-3}, [Hg (OAc)$_2$] = 5.00×10^{-3} mol dm^{-3} and AcOH–H$_2$O = 1:1% (v/v)

Reported rate constants are the mean of duplicate experiments

Table 3 Temperature dependence and activation parameters for the Ru(III)-catalyzed and uncatalyzed oxidation of 4-oxo acids by bromate in acid medium

4-oxo acid	$10^5 \times k$ (s^{-1})						E_a (kJ mol^{-1})	$\Delta H^{\#}$ (kJ mol^{-1})	$\Delta S^{\#}$ (J mol^{-1} K^{-1})	$\Delta G^{\#}$ (kJ mol^{-1})
	298	303	308	313	318	323 K				
–H	47.97	73.31	95.95	127.94	191.91	338.22	68.92	66.30	−89.06	96.79
	(0.39)[a]	(0.70)	(1.35)	(3.19)	(4.79)	(9.59)	(101.46)	(98.87)	(80.26)	(73.74)
p-OCH$_3$	639.22	767.66	959.58	1,151.15	1,279.41	1,599.18	38.29	35.69	−168.5	88.45
	(14.43)	(19.19)	(28.78)	(47.97)	(57.57)	(67.17)	(47.86)	(45.26)	(−68.32)	(66.64)
p-CH$_3$	11.15	159.93	223.88	287.87	447.72	639.54	57.44	54.84	−118.8	92.04
	(1.13)	(1.91)	(3.19)	(6.71)	(11.19)	(17.61)	(76.86)	(73.96)	(−69.47)	(71.79)
p-Cl	19.29	31.90	43.61	79.96	134.34	223.80	82.33	79.73	−49.9	95.36
	(0.26)	(0.39)	(0.71)	(1.06)	(1.72)	(3.59)	(114.85)	(112.25)	(9.5)	(70.98)
m-NO$_2$	2.98	5.75	9.59	17.58	223.80	63.90	105.30	102.70	10.7	99.34
	(–)	(–)	(0.17)	(0.37)	(3.59)	(1.43)	(134.09)	(131.49)	(66.27)	(76.21)

Solution conditions: [Oxo acid] = 1.00×10^{-2} mol dm^{-3}, [bromate] = 1.00×10^{-3} mol dm^{-3}, mol dm^{-3}, [Ru(III)] = 3.3×10^{-5} mol dm^{-3}, [H$_2$SO$_4$] = 1.00 mol dm^{-3}, [Hg (OAc)$_2$] = 5.00×10^{-3} mol dm^{-3} and AcOH–H$_2$O = 1:1% (v/v)

The average error in values of E_a, $\Delta H^{\#}$, $\Delta S^{\#}$ and $\Delta G^{\#}$ are ± 1.6 kJ mol^{-1}, ±1.6 kJ mol^{-1}, ± 3 J mol^{-1} K^{-1} and ± 2 kJ mol^{-1}, respectively. $\Delta H^{\#}$, $\Delta S^{\#}$ and $\Delta G^{\#}$ values were obtained at 313 K. The average error in rate constant is ±5%

[a] Parentheses values indicate the rate constants (k_{un}, s^{-1}) and activation parameters of uncatalyzed reactions

decreases in magnitude with increase in temperature (−1.47, −1.33, −1.28, −1.10 and −1.02 at 303, 308, 313, 318 and 323 K, respectively). The reaction constant, or sensitivity constant, ρ^+, describes the susceptibility of the reaction to substituents and is a measure of the extent of electron demand at the seat of reaction. The negative ρ^+ value in the present study indicates that positive charge builds up in the transition state. As the value of ρ^+ is related to the charge during the rate-determining step (k_d), it decreases with increase in temperature.

Stoichiometry and product analysis

Reaction mixtures containing different ratios of [bromate] to [oxo acid] in the presence of the requisite amounts of other reagents were equilibrated at 40 °C for 12 h. The unreacted [bromate] was determined by iodometry. The results (Table 4) clearly demonstrate the consumption of 7 moles of bromate for 3 moles of the oxo acid. This stoichiometry, together with the detection of benzoic acid, bromide and CO$_2$ in the product analysis, indicates the following stoichiometric equation:

The same stoichiometry was observed with all the studied 4-oxo acids. Benzoic acid, after separation by HPLC (m.p. 121 °C), was estimated quantitatively (92–96% yield) with a standard curve at 235 nm (λ_{max}). CO$_2$ was identified by bubbling N$_2$ gas through the reaction mixture and passing the liberated gas through a U-shaped tube containing a saturated Ba(OH)$_2$ solution. Formation of a white precipitate of BaCO$_3$ indicated the liberation of CO$_2$. A test for the formation of Br$^-$ was carried out by adding silver nitrate solution to the reaction mixture after completion of the reaction. The pale yellow precipitate of silver bromide confirmed the formation of bromide as one of the products of the reaction. No molecular bromine was observed in these experiments.

On the basis of the observed kinetic orders, the rate law can be expressed as:

$$\frac{-\mathrm{d[bromate]}}{\mathrm{d}t} = k[\text{bromate}][\text{H}^+][\text{oxo acid}]^x [\text{Ru(III)}]^y \quad (2)$$

where x and y are less than unity and this equation holds good for both oxo acid and Ru(III) in the studied concentration range.
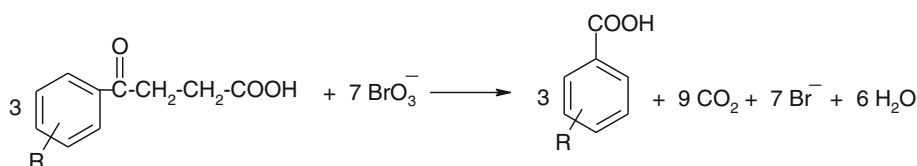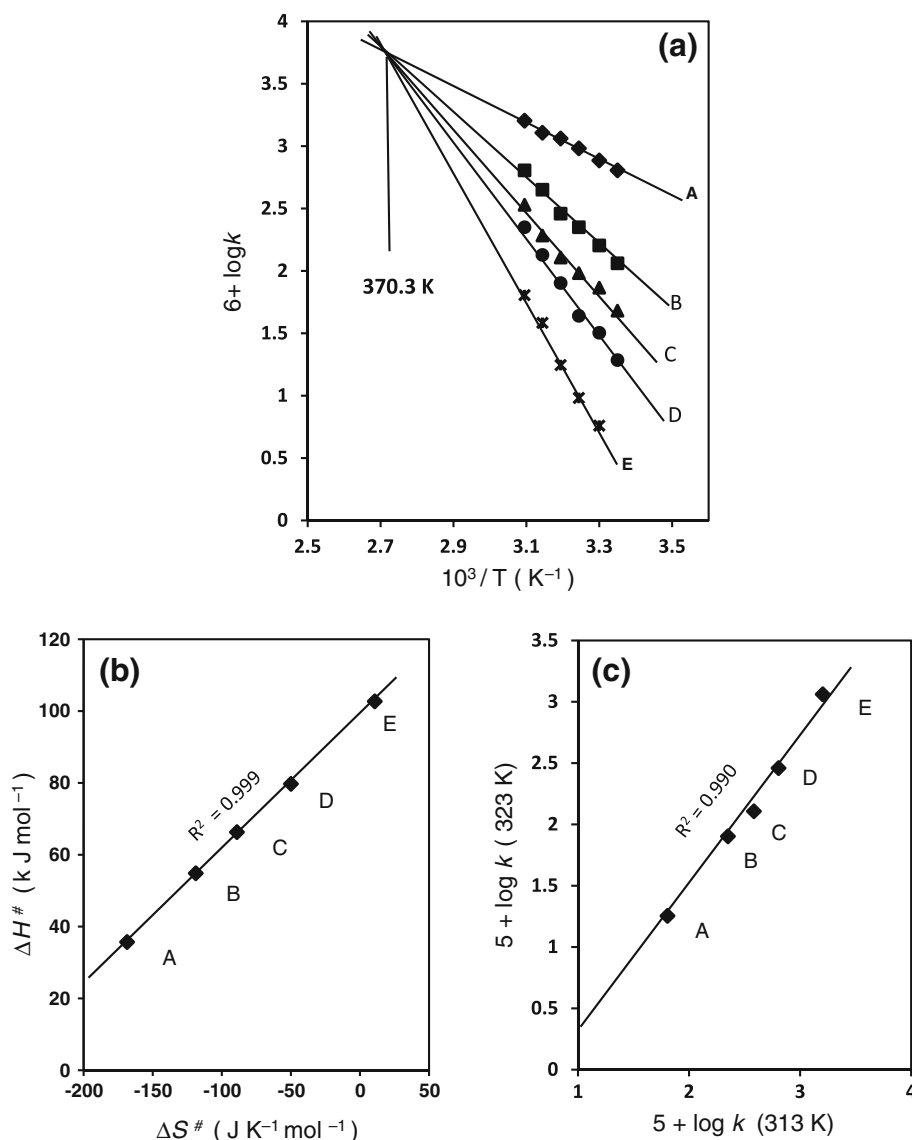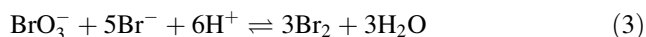
Discussion

Role of mercury(II) acetate

The presence of mercury(II) (in excess of bromate concentration) simply means that Br_2 oxidation is completely suppressed; Br_2 otherwise would have been formed by the interaction between bromate and bromide (the reduction product of bromate) as:

$$BrO_3^- + 5Br^- + 6H^+ \rightleftharpoons 3Br_2 + 3H_2O \qquad (3)$$

No free radicals were observed in these reactions, and the reaction rates were independent of [Hg]. These considerations confirm that Hg(II) acts only as a scavenger [11, 14] for any bromide formed, forming $HgBr^+$ ($K_1 = 2.51 \times 10^8$ $dm^3\ mol^{-1}$) and $HgBr_2$ ($K_2 = 3.80 \times 10^8$ $dm^3\ mol^{-1}$) and

ensuring that the oxidation takes place purely through bromate.

Acetate ion catalysis in the bromate–bromide reaction was reported by Cortes and Faria [17], and the experimental results were interpreted in a six-term rate law, with and without involvement of acetate ion. The mechanism proposed considers that when acetate binds to bromate, it facilitates its second protonation. However, in the present study, no catalytic effect of acetate was observed when mercury acetate was added to the reaction mixture over a wide concentration range (0.001–0.01 mol dm^{-3}).

Identification of reactive species

Potassium bromate is a strong electrolyte, and in aqueous solution, it exists as BrO_3^- ion, which is a very weak base
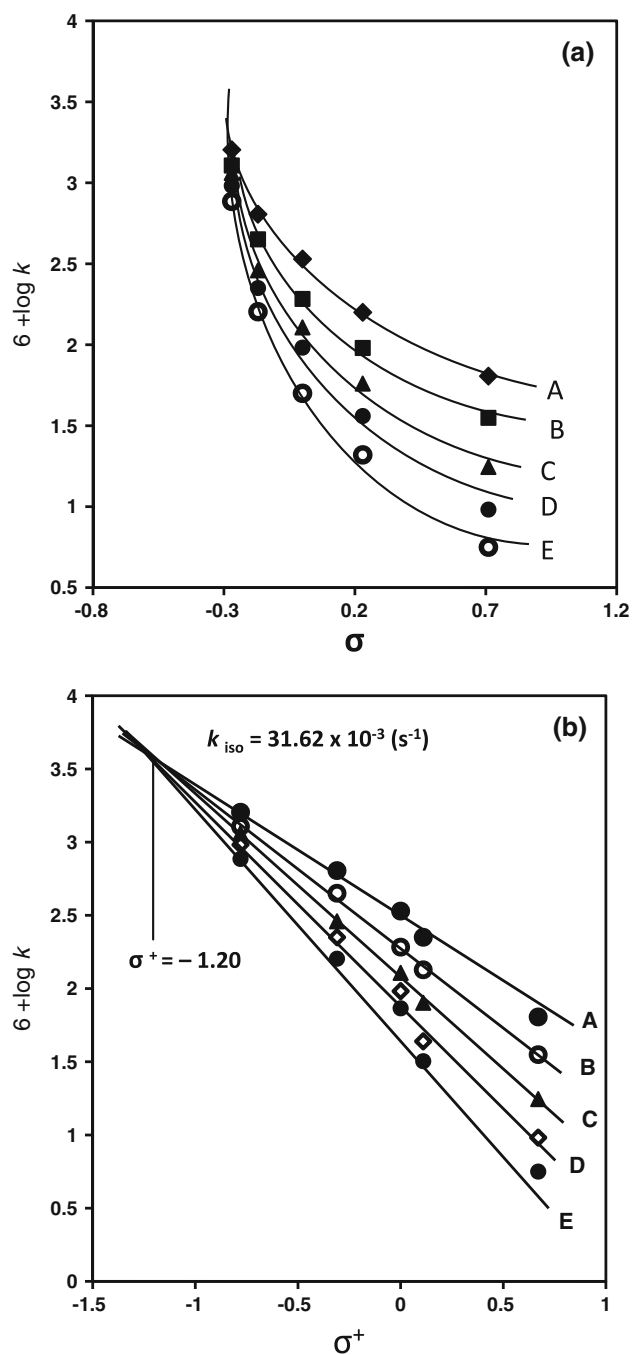
Fig. 5 a Hammett plots of log k against σ at different temperatures. **b** Hammett plots of log k against σ^+ at different temperatures. Reaction conditions as in Table 3. *A* 323 K, *B* 318 K, *C* 313 K, *D* 308 K, *E* 303 K

Table 4 Consumption of bromate in the oxidation of 4-oxo acid

[Oxo acid] × 10^3 (mol dm^{-3})	[Bromate] × 10^3 (mol dm^{-3})			[Bromate]: [Oxo acid]
	Initial	Final	Consumed	
1.0	10	7.67	2.33	2.33
2.0	20	15.35	4.67	2.32
5.0	50	38.26	11.74	2.35

Solution conditions: [Ru(III)] = 3.3×10^{-5} mol dm^{-3}, [H$_2$SO$_4$] = 1.00 mol dm^{-3}, [Hg(OAc)$_2$] = 5.00×10^{-3} mol dm^{-3} and AcOH–H$_2$O = 1:1% (v/v), Temp. 313 K

A study on oxidation states of Ru has shown [19–22] that Ru(III) undergoes the following equilibria in acid medium.

$$RuCl_3 + 3HCl \rightleftharpoons [RuCl_6]^{3-} + 3H^+ \tag{4}$$

$$[RuCl_6]^{3-} + H_2O \rightleftharpoons [RuCl_5(H_2O)]^{2-} + Cl^- \tag{5}$$

From ion-exchange studies, it is confirmed that RuCl$_3$ forms [RuCl$_6$]$^{3-}$ in hydrochloric acid [19], and aquation of these species to form [RuCl$_5$(H$_2$O)]$^{2-}$ requires only a few seconds [20–22]. Therefore, it is assumed that Ru(III) in the form of [RuCl$_5$(H$_2$O)]$^{2-}$ is taking part in the reaction. The negative effect of Cl$^-$ ion on the rate of reaction is also in support of this assumption. The same species was also assumed to be the reactive catalyst in Ru(III)-catalyzed oxidations of various organic substrates by different oxidants [8, 23–25] in acid medium. In acid solutions, [RuCl$_5$(H$_2$O)]$^{2-}$ shows an absorption maximum (λ_{max}) of 490 nm. Neither bromate nor the 4-oxo acid has λ_{max} in this region. A change in λ_{max} and the absorption of Ru(III), on the addition of oxo acid (in the absence of bromate), indicate the formation of a complex between Ru(III) and the oxo acid, which is likely to be an outer sphere complex. There is no absorption at 690 nm, which is characteristic of Ru(V) species. Formation of the complex was also implicated by a non-zero intercept in the plot of $1/k$ versus $1/$[oxo acid] (Fig. 1). Similar complex formation between organic substrates and Ru(III) has been observed in the literature [8, 23–25]. The uncatalyzed acid bromate oxidation of 4-oxo acids was first order in both [oxo acid] and [bromate], and $1/k_{un}$ versus $1/$[oxo acid] plots were linear passing through origin. The apparent fractional order with respect to [Ru(III)] and a definite intercept in the $1/k$ versus $1/$[Ru(III)] plots (Fig. 3) are further evidence for complex formation between the oxo acid and Ru(III), which subsequently reacts with bromate. The 4-oxo acids are weak acids with pK_a of 5.77 in aqueous solution at 40 °C [26]; hence, in acid medium, they will exist in the undissociated form. 4-Oxo acids enolize in acid medium.
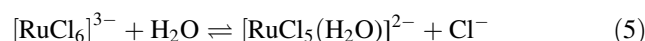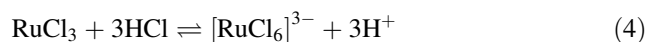
[17]. HBrO$_3$ is a very strong acid [18] and its protonation to H$_2$BrO$_3^+$ is not significant under our experimental conditions. Hence, in the present experiments, BrO$_3^-$ is assumed to be the main reactive species of the oxidant and the involvement of HBrO$_3$ or H$_2$BrO$_3^+$ can be excluded.

Scheme 1 Reaction mechanism for the oxidation of 4-oxo acids by bromate in the presence of Ru(III)
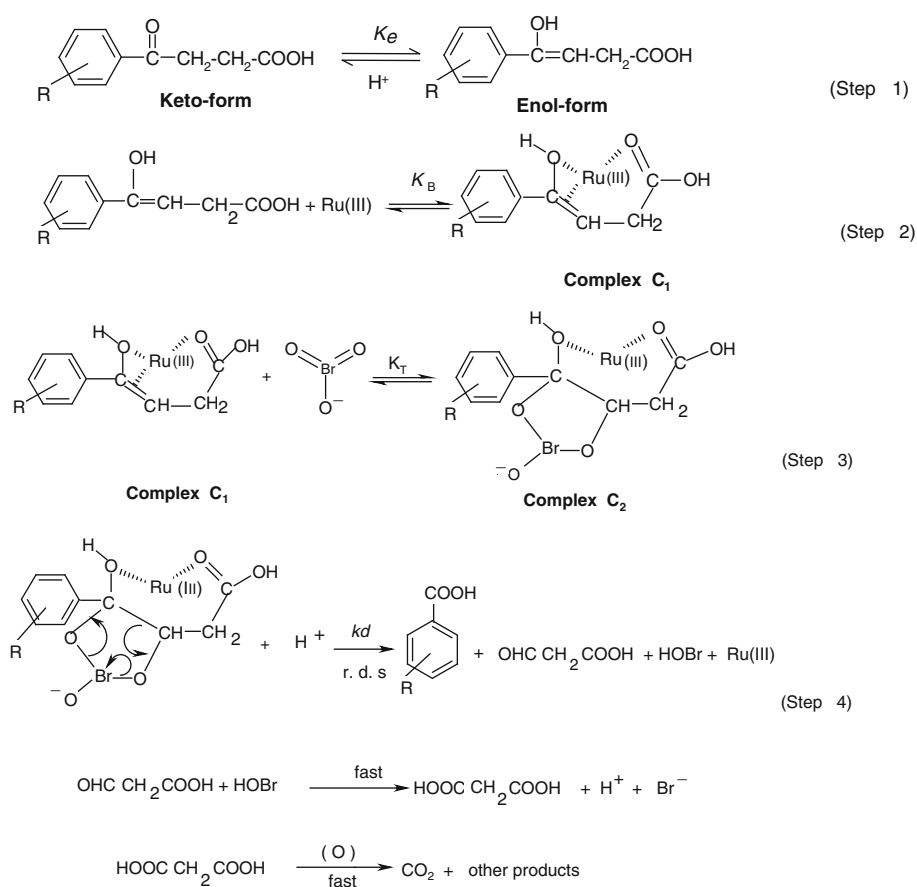
Reaction mechanism

The observed stoichiometry and effects of various parameters on the kinetics of this reaction allow us to propose a mechanism as in Scheme 1.

The rate of enolization (determined by the bromination method) is greater than the rate of oxidation by a factor of ca. 15–18; hence, the step involving enol formation will not be the rate-determining step and the reaction may be visualized as proceeding via the enol form of the oxo acid.

In our proposed mechanism, the active species of Ru(III) forms an outer sphere complex with the enol form of the oxo acid (complex C_1). The alkene, –OH and –COOH groups could all be involved in complex formation with the transition metal. Although evidence for specific interactions was not obtained, the spectroscopic evidence for formation of such a complex was obtained from the UV–visible spectra of the catalyst, compared with a mixture of catalyst and oxo acid in acid medium. A bathochromic shift from 490 to 496 nm, with hyperchromic shift in the molar extinction coefficient of the Ru(III) solution in the presence of oxo acid, was obtained. Formation of the complex was also implicated by a non-zero intercept in the plots of $1/k$ against $1/$[oxo acid] and $1/k$ against $1/$[catalyst]. Bromate

then reacts with the binary complex C_1, giving a cyclic bromate ester (ternary complex C_2). The concerted cis 1,3-cycloaddition of BrO_3^- to the carbon–carbon double bond of the substrate has also been proposed in the bromate oxidation of cinnamic acids [27] and in the pyridinium fluorochromate oxidation of 4-oxo acids [28]. Ru(III) ene π-complex formation enhances the reactivity of the C=C of complex C_1 to form the cyclic bromate ester. The decomposition of the five-membered ring complex C_2 involving C–C and O–Br bonds (in the rate-determining step), results in benzoic acid and formyl acetic acid, and the oxidation state of Ru(III) is unaltered during the course of the reaction. This is consistent with the fact that no Ru(V) ($\lambda_{max} = 690$ nm) or Ru(I) species were observed by uv–vis. during the reaction. The formyl acetic acid on oxidation with the HOBr product converts into malonic acid along with the formation of Br^- ion, further reactions giving CO_2 and H_2O as final products. The intermediates formed during the oxidation of malonic acid were identified by HPLC and by various tests [11]. The proposed mechanism is also in accordance with the observed stoichiometry. This mechanism is an example for the neighboring group participation with intramolecular catalysis of Ru(III) in the oxidation of 4-oxo acids.

Rate law and verification

On the basis of the reaction in Scheme 1, the rate in terms of decrease in concentration of bromate can be expressed as Eq. 6;

$$\frac{-d[BrO_3^-]}{dt} = kd[\text{Complex } C_2][H^+] \tag{6}$$

On the basis of the equilibrium steps in Scheme 1, Eqs. 7 and 8 can be obtained as follows:

$$[\text{Complex } C_1] = K_B Ke[\text{Oxo acid}][\text{Ru(III)}] \tag{7}$$

$$[\text{Complex } C_2] = K_T K_B Ke[\text{Oxo acid}][\text{Ru(III)}][BrO_3^-] \tag{8}$$

With the help of Eqs. 6–8, we can write Eq. 9 as

$$\frac{-d[BrO_3^-]}{dt} = kd K_T K_B Ke[\text{Oxo acid}][\text{Ru(III)}][BrO_3^-][H^+] \tag{9}$$

Since, bromate is present in complexed and uncomplexed forms, at any time the total concentration of bromate can be given as

$$[Br(V)]_T = [BrO_3^-] + [\text{Complex } C_2] \tag{10}$$

$$[Br(V)]_T = [BrO_3^-] + K_T K_B Ke[\text{Oxo acid}][\text{Ru(III)}][BrO_3^-] \tag{11}$$

$$[Br(V)]_T = [BrO_3^-] + [1 + K_T K_B Ke[\text{Oxo acid}][\text{Ru(III)}]] \tag{12}$$

Therefore,

$$[BrO_3^-] = \frac{[Br(V)]_T}{1 + K_T K_B Ke[\text{Oxo acid}][\text{Ru(III)}]} \tag{13}$$

The rate law in terms of total bromate concentration can then be given as

$$\frac{-d[Br(V)]_T}{dt} = \frac{kd K_T K_B Ke[H^+][\text{Oxo acid}][\text{Ru(III)}][Br(V)]_T}{1 + K_T K_B Ke[\text{Ru(III)}][\text{Oxo acid}]} \tag{14}$$

The rate law (Eq. 14) is in accordance with the experimental results, wherein a first-order dependence on both [bromate] and [acid], and fractional orders in both [oxo acid] and [catalyst] were observed.

The rate law (Eq. 14) may be rearranged to Eqs. 15–17, which are suitable for verification.

$$\frac{\text{Rate}}{[Br(V)]_T} = k = \frac{kd K_T Ke[H^+][\text{Ru(III)}][\text{Oxo acid}]}{1 + K_T K_B Ke[\text{Ru(III)}][\text{Oxo acid}]} \tag{15}$$

$$\frac{1}{k} = \left[\frac{1}{kd K_T K_B Ke[\text{Ru(III)}][\text{Oxo acid}]} + \frac{1}{kd} \right] \frac{1}{[H^+]} \tag{16}$$

At constant acid (1.0 mol dm^{-3}) concentration, Eq. 16 reduces to Eq. 17.

$$\frac{1}{k} = \frac{1}{kd K_T K_B Ke[\text{Ru(III)}][\text{Oxo acid}]} + \frac{1}{kd} \tag{17}$$

According to Eq. 16, other conditions being constant, a plot of $1/k$ versus $1/[H^+]$ should be linear passing through the origin and the same is observed (Fig. 3). Similarly, according to Eq. 17, plots of $1/k$ versus $1/[\text{oxo acid}]$ (at constant [Ru(III)]) and $1/k$ against $1/[\text{Ru(III)}]$ (at constant [oxo acid]) should be linear with a definite intercept on the $1/k$ axis. These observations (Figs. 1, 2) support the validity of the rate law (Eq. 14). The proposed mechanism is further supported by the solvent influence on the reaction rate. The intermediate complex C_2 is less polar than the reactants due to dispersal of charge, and hence, decreasing polarity of the solvent is expected to stabilize complex C_2 in preference to the reactants, thereby enhancing the reaction rate. Such a solvent influence has indeed been observed (Table 1). The positive values of the free energy and enthalpy of activation indicate that the transition state is highly solvated, while the negative entropy of activation suggests the formation of a compact activated complex with fewer degrees of freedom.

From the intercept and slope data of Figs. 1 and 2, the decomposition constant (kd), and enolization and complexation constants (Ke and $K_B K_T$) have been evaluated and the values are presented in Table 5.

Structural influences and linear free-energy relationships

The order of reactivity among the phenyl substituted 4-oxo acids is p-methoxy $\gg$ p-methyl > –H > p-chloro > m-nitro oxo acid. A plot of log k versus Hammett's sigma values gave a smooth curve at all the studied temperatures (Fig. 5a). The curvature may be attributed to (1) a gradual change in the reaction mechanism when one passes from

Table 5 Evaluated decomposition constant (kd), enolization and formation constants (KeK_BK_T) of Ru(III)-catalyzed oxidation of 4-oxo acids at 313 K using Eq. 17

Substituent	$kd \times 10^3$ s^{-1} (decomposition constant)	$KeK_BK_T \times 10^{-5}$ (formation constants)
p-OCH$_3$	22.72	37.42
p-CH$_3$	6.90	25.69
–H	3.12	22.28
p-Cl	1.64	21.37
m-NO$_2$	0.45	21.06

Solution conditions: [Oxo acid] = 1.00×10^{-2} mol dm^{-3}, [bromate] = 1.00×10^{-3} mol dm^{-3}, [Ru(III)] = 3.3×10^{-5} mol dm^{-3}, [H$_2$SO$_4$] = 1.00 mol dm^{-3}, [Hg (OAc)$_2$] = 5.00×10^{-3} mol dm^{-3} and AcOH–H$_2$O = 1:1% (v/v)

The average error in kd and KeK_BK_T values is $\pm 5\%$

electron-donating to electron-withdrawing substituents, (2) a change in the rate-determining step or (3) a change in the nature of transition state. The linearity of the Exner's plot (Fig. 4c) suggests that these reactions follow a similar mechanism [29]. The isokinetic temperature (β) was calculated as 370.2 K from the slope of the plot of log k at 323 K against log k at 313 K (Fig. 4c), indicating that the rate is governed by the enthalpy of activation. This is also corroborated by near constancy in $\Delta G^{\#}$ values.

From the preceding discussion, it may be construed that the curve in plot of log k versus σ (Fig. 5a) is a result of the change in the nature of the transition state when one goes from electron-releasing to electron-withdrawing substituents, i.e., an electronic perturbation effect. The transition state (Scheme 1) involves both C–C bond cleavage and C–O bond formation. If both the steps are influenced in the same way by the substituents, a linear Hammett plot is expected. However, if the two processes influence the reaction in different ways, a curved Hammett plot will be obtained. Electron-releasing substituents may lead to a transition state, in which C–C bond-breaking has progressed to a greater extent than the C–O bond formation, while the converse would be true for electron-attracting substituents. The activation parameters are in favor of this view. The $\Delta H^{\#}$ value is seen to decrease with increasing electron-donating ability of the substituents (Table 3), whereas, $\Delta S^{\#}$ becomes more negative, reflecting a more solvated transition state. For electron attractors like the nitro group, bond formation is apparently more important, since $\Delta H^{\#}$ increases, resulting in decreased rate of solvolysis, while $\Delta S^{\#}$ becomes positive. Higher values of sigma, i.e., exalted Brown and Okamoto's σ^{+} values [16] can be used to give linear correlations. This is observed in the present study; a plot of log k versus σ^{+} was linear with a slope of −1.28 at 313 K (Fig. 5b). The reaction constant (ρ^{+}), which is a measure of the extent of electron demand at the seat of reaction, decreases in magnitude with increase in temperature. The negative value of ρ^{+} suggests the sensitivity of the reaction to the effects of electronic perturbation. It also provides information about the nature of the transition state. A reaction involving positive charge development in the transition state is aided by electron-releasing substituents and the ρ^{+} value will be negative [30], as in the present case. The ρ^{+} value (−1.02 to −1.47) in the present study may be attributed to the nature of the observed rate constant (k), which is a composite of several terms like enolization, complexation, oxidation, etc.

The effect of various substituents on the reaction rate is as expected, with the exception of p-methoxy, which showed a significant increase in the rate. This may be explained on the basis of the σ values of the methoxy substituent. The σ_m value for methoxy is +0.115, while σ_p is −0.268. These values show that the methoxy group

decreases the rate of oxidation of meta-substituted compounds through the inductive effect. But the mesomeric effect in para-substituted compounds overweighs the inductive effect, resulting in overall electron release to the aromatic ring. Thus, in the oxidation of p-methoxy 4-oxo-4-phenylbutanoic acid, direct mesomeric interaction with the reaction center also comes into play, resulting in greater electron release than expected on the basis of the Hammett σ value.

Isokinetic relationships and catalytic efficiency

The Hammett reaction constant (ρ^{+}) decreases in magnitude with increase in temperature, from −1.47 at 303 K to −1.02 at 323 K. This indicates that the carbocationic character of the transition state decreases with increase in temperature. At the isokinetic temperature, ρ^{+} becomes zero, and there is no sensitivity to substituents. The Hammett lines intersect at a point corresponding to an σ_{iso}^{+} value of −1.20 and a k_{iso} value of 31.62×10^{-3} s^{-1} (Fig. 5b).

A reaction series that exhibits a common point of intersection in the Hammett plot (Fig. 5b), is expected to have a common point of intersection in the Arrhenius plot also [29]. The Arrhenius plots are shown in Fig. 4a. From the plots of $\Delta H^{\#}$ against $\Delta S^{\#}$ (Fig. 4b) and ρ^{+} against $1/T$ (Fig. 6), according to the equation

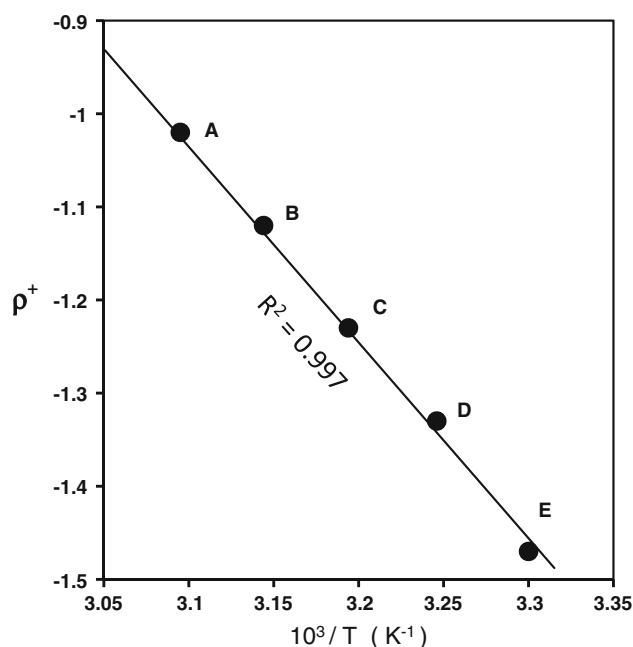$$\rho = \rho^{\alpha}(1 - \beta/T) \tag{18}$$

Fig. 6 Plot between ρ^{+} and $1/T$ at different temperatures. Reaction conditions as in Table 3. A 323 K, B 318 K, C 313 K, D 308 K, E 303 K

Table 6 Values of catalytic constant (K_C) at different temperatures and activation parameters calculated using K_C value

4-oxo acid	$K_C \times 10^2$						E_a (kJ mol^{-1})	$\Delta H^{\#}$ (kJ mol^{-1})	$\Delta S^{\#}$ (J mol^{-1} K^{-1})	$\Delta G^{\#}$ (kJ mol^{-1})
	298	303	308	313	318	323 K				
–H	8.35	12.77	16.71	22.28	33.43	58.92	53.16	51.01	−94.9	80.72
p-OCH$_3$	111.11	133.70	167.1	200.5	222.8	(–)	29.45	26.85	−153.8	75.01
p-CH$_3$	20.06	27.80	39.12	50.15	78.02	111.45	58.50	55.90	−72.7	78.66
p-Cl	3.33	5.55	7.59	13.91	23.40	38.98	80.84	78.24	−11.8	60.4
m-NO$_2$	0.51	1.00	1.67	3.00	6.12	11.11	107.51	104.91	60.4	85.98

Solution conditions: [Oxo acid] $= 1.00 \times 10^{-2}$ mol dm^{-3}, [bromate] $= 1.00 \times 10^{-3}$ mol dm^{-3}, mol dm^{-3}, [Ru(III)] $= 3.3 \times 10^{-5}$ mol dm^{-3}, [H$_2$SO$_4$] $= 1.00$ mol dm^{-3}, [Hg (OAc)$_2$] $= 5.00 \times 10^{-3}$ mol dm^{-3} and AcOH–H$_2$O = 1:1% (v/v)

The average error in values of E_a, $\Delta H^{\#}$, $\Delta S^{\#}$ and $\Delta G^{\#}$ are ± 1.6 kJ mol^{-1}, ± 1.6 kJ mol^{-1}, ± 3 J mol^{-1} K^{-1} and ± 2 kJ mol^{-1}, respectively. $\Delta H^{\#}$, $\Delta S^{\#}$ and $\Delta G^{\#}$ values were obtained at 313 K. The average error in the catalytic constant is $\pm 5\%$

The T_{iso} value is 369.0 K, in good agreement with the value of 370.2 K obtained from the Exner's plot (Fig. 4c).

Moelwyn-Hughes [31] pointed out that when catalyzed and uncatalyzed reactions proceed simultaneously, the relationship is given as:

$$k_{obs} = k_{un} + K_C[\text{catalyst}]^y \quad (19)$$

where k_{obs} is the observed pseudo-first-order rate constant obtained in the presence of Ru(III) catalyst, k_{un} is that for the uncatalyzed reaction, K_C is the catalytic constant and y is the order of the reaction with respect to [Ru(III)], which is 0.5 in the present study. The value of K_C was calculated using the equation

$$K_C = (k_{obs} - k_{un})/[\text{Ru(III)}]^{0.5} \quad (20)$$

The values of K_C were calculated at different temperatures (298–323 K), and a plot of log K_C versus $1/T$ was linear ($R^2 \geq 0.993$). The energy of activation and other thermodynamic parameters for the catalyst are tabulated in Table 6. The high K_C value indicates that Ru(III) is an efficient catalyst in the bromate oxidation of 4-oxo acids.

Finally, we have compared our findings with those reported for the osmium(VIII) catalyzed oxidation of oxo acids by alkaline hexacyanoferrate(III). The proposed mechanism in this case involves rapid complex formation between the enolate anion of the 4-oxo acid and [OsO$_4$-(OH)$_2$]$^{2-}$, which decomposes into products in the slow step giving Os(VI). The Os(VI) is reoxidized to Os(VIII) by [Fe(CN)$_6$]$^{3-}$ in a fast step [32]. On the other hand, in the alkaline hexacyanoferrate(III) oxidation of 4-oxo acids, a mechanism involving the formation of enolate anion from the oxo compound and subsequent rate-determining electron transfer by the oxidant has been proposed [33]. In the present investigation, the experimental results are entirely different from the earlier reports and a different mechanism wherein neighboring group participation in the intramolecular catalysis is proposed.

Conclusion

From the Hammett and Arrhenius plots associated with isokinetic relationships, the ρ^+ values are negative and decrease with increasing temperature. Electron donors accelerate the reaction rate and electron acceptors retard it. The structure-reactivity correlations suggest a carbocationic reaction center in the transition state. It may be concluded that Ru(III) acts as an efficient catalyst in the oxidation of 4-oxo acids by bromate in acid medium. Unlike earlier studies, this reaction is an example of the neighboring group participation and intramolecular catalysis and is a valuable protocol for the synthesis of substituted benzoic acids.

References

1. Bell RB, Covington D (1975) J Chem Soc Perkin Trans 2:1343–1348
2. Fadnavis NW, Bhagavant G (1979) Ind J Chem 17B:518–525
3. Bhatt MV, Ravindranathan MS, Rao GV (1984) J Org Chem 49:3170–3176
4. Mohamed Farook NA (2006) J Iranian Chem Soc 3:378–386
5. Ju Lurie (1975) Hand book of analytical chemistry. Mir Publishers, Moscow, pp 301–302
6. Jonnalagadda SB, Shezi M, Pare B (2003) Int J Chem Kinet 35:294–298
7. Muceintes AE, Gabaldon RE, Poblete FJ, Villarreal S (2004) J Phys Org Chem 17:236–239
8. Puttaswamy, Pranesh Shubha J (2008) Trans Met Chem 33: 1003–1011
9. Singh AK, Negi R, Katre YR (2009) J Mol Catal A Chem 320: 36–42, and the references therein
10. Singh AK, Jain B, Negi R, Katre YR, Singh SP, Sharma VK (2010) Trans Met Chem 35:407–414

11. Sanjeeva Reddy Ch, VijayaKumar T (2007) Trans Metal Chem 32:246–256
12. Jonnalagadda SB, Chinake C, Simoyi RH (1995) J Chem Soc Faraday Trans 91:1635–1640
13. Houricichi YC, Osmu C (1970) Chem Abstr 72:50624
14. Bailar JC (1956) The chemistry of coordination compounds. Reinhold, New York, p 14
15. Collins CJ, Bowman NS (1970) Isotope effects in chemical reactions. Van Nostrand Reinhold, New York, p 267
16. Brown HC, Okamoto Y (1958) J Am Chem Soc 80:4079–4987
17. Cortes CES, Faria RD (2004) Inorg Chem 43:1395–1402
18. Alves WA, Tellez CA, Sala O, Santos PS, Faria RB (2001) J Raman Spectrosc 32:1032–1036
19. Connick RE, Fine DA (1961) J Am Chem Soc 83:3414–3418
20. Taqui Khan MM, Chatterjee D, Bhatt SD, Rao AP (1992) J Mol Catal 77:23–28
21. Davfokratova T (1963) Analytical Chemistry of ruthenium. Academy of Sciences, USSR, pp 54, 71 and 97
22. Griffith WP (1967) The chemistry of rare platinum metals. Interscience, New York, p 141
23. Singh B, Singh AK, Singh NB, Saxena BBL (1984) Tetrahedron 40:5203–5206
24. Singh B, Singh PK, Singh D (1988) J Mol Catal 78:207–215
25. Singh MP, Singh HH, Verma MK (1980) J Phys Chem 84:256–259
26. Sikkandar G, Basheer Ahamed KA (1999) Ind J Chem 38A: 183–186
27. Sanjeeva Reddy Ch, Sundaram EV (1989) Tetrahedron 45: 2109–2126
28. Kavitha S, Pandurangan A, Alphonse I (2005) Ind J Chem 44A: 715–718
29. Schmid R, Sapunov VN (1982) Non-formal kinetics. In: Ebel HF (ed) Monograph in modern chemistry. Verlag, Chemie, Weinheim, p 21
30. Ruff F, Kucsman AJ (1985) J Chem Soc Perkin Trans 2:683–687
31. Moelwyn-Hughes EA (1947) Kinetics of reactions in solutions. Oxford University press, London, pp 297–299
32. Gnana Rani DF, Maria Pushparaj FJ, Alphonse I, Rangappa KS (2002) Ind J Chem 41B:2153–2159
33. Maria Pushparaj FJ, Kannan S, Vikram L, Lalitha SK, Rangappa KS (2005) J Phys Org Chem 18:1042–1049